J|A|C|S COMMUNICATIONS

Published on Web 12/17/2010

Dynamics of Simultaneous, Single Ion Transport through Two Single-Walled Carbon Nanotubes: Observation of a Three-State System

Wonjoon Choi,[†,‡] Chang Young Lee,[†] Moon-Ho Ham,[†] Steven Shimizu,[†] and Michael S. Strano*[,†]

Departments of Chemical and Mechanical Engineering, Massachusetts Institute of Technology, Cambridge, Massachusetts 02139, United States

Received September 14, 2010; E-mail: strano@mit.edu

Abstract: The ability to actively manipulate and transport single molecules in solution has the potential to revolutionize chemical synthesis and catalysis. In previous work, we developed a nanopore platform using the interior of a single-walled carbon nanotube (diameter = 1.5 nm) for the Coulter detection of single cations of Li^+, K^+, and Na^+. We demonstrate that as a result of their fabrication, such systems have electrostatic barriers present at their ends that are generally asymmetric, allowing for the trapping of ions. We show that above this threshold bias, traversing the nanopore end is not rate-limiting and that the pore-blocking behavior of two parallel nanotubes follows an idealized Markov process with the electrical potential. Such nanopores may allow for high-throughput linear processing of molecules as new catalysts and separation devices.

The ability to actively manipulate and transport single molecules in solution has the potential to revolutionize chemical synthesis and catalysis. While silicon nanopores, for example, have been used to capture and translocate DNA and proteins,[1−4] these nanopores have diameters that are too large and aspect ratios that are too low to detect and manipulate small organic or inorganic molecules.[5,6] We recently developed a nanopore platform using the interior of a single-walled carbon nanotube (SWNT; diameter = 1.5 nm) that demonstrates the detection of single cations of Li^+, K^+, and Na^+.[7] By entering the nanotube, these species interrupt an otherwise constant proton current that traverses the conduit.[7,8] In this work, we focus on the utilization of this system to carry the target ion as a precursor to subsequent chemistry using potential barriers from charged carboxylic acid groups[9] at the two ends of the nanotube pore. We show that above a threshold bias, traversing the nanopore ends is not rate-limiting and that the pore-blocking behavior of two parallel nanotubes follows an idealized Markov process with the electrical potential. Such nanopores may allow for high-throughput linear processing of molecules as new catalysts and separation devices.

The platform was constructed using an epoxy structure that acts as both an oxygen plasma mask for the opening of the nanotube ends and a barrier between two liquid reservoirs, one on either side.[7] The SWNTs were synthesized and aligned using methane chemical vapor deposition (CVD) (Figure S1 in the Supporting Information).[10] The plasma etch removed exposed SWNTs, leaving 1 mm across the protected section, and opened the two ends at the bottoms of the epoxy reservoirs (Figure 1a). An electrolyte solution (3 M KCl) was placed in both wells, and Ag/AgCl electrodes were used

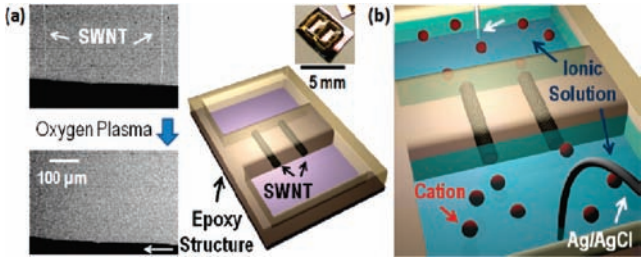

Figure 1. Schematic of SWNT ion channel device. (a) Ultralong SWNTs are aligned on a silicon wafer, and an epoxy structure is attached to the wafer by UV glue to cover the SWNTs during etching. (b) The epoxy structure also acts as a barrier between the two ionic solutions, blocking all molecular transport except that through the SWNTs.

with a voltage clamp to detect the translocation of single ions (Figure 1b). An applied bias between 0 and 695 mV (Figure S2) resulted in only a flat baseline current, which was previously demonstrated to be due to proton transport from the anode to the cathode. Notably, increasing the bias to 800 mV clearly showed the onset of pore blocking. The cations of KCl were previously shown to be the dominant pore blockers under these conditions.[7] Through a progressive bisection of the interval spanning the blocking and nonblocking conditions, an estimate of the threshold potential for pore blocking could be made. Figure 2a shows that

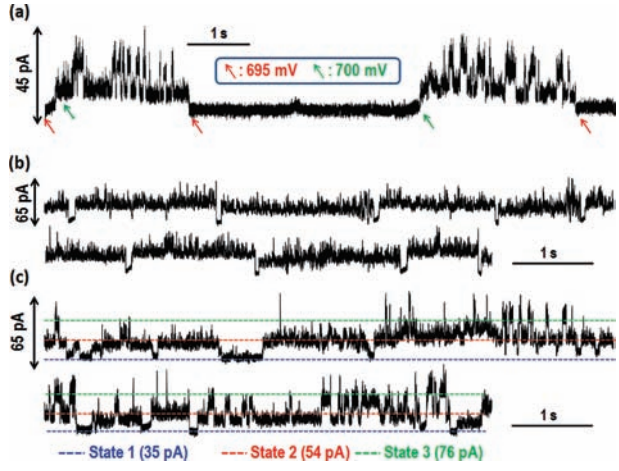

Figure 2. (a) Threshold voltage (700 mV) of blockade current by ion transport. (b) Stochastic pore blocking through SWNT #2 (800 mV). Among stochastic events, pore-blocking events having short dwell times occur in SWNT #1. (c) Proof of two activated SWNTs in ion channels (800 mV). The blockade current shows three states, indicating a system of two pores.

cycling between 695 and 700 mV resulted in nonblocking and stochastic blocking intervals, respectively, in the current trace. This threshold yielded the electrostatic barrier for K^+ partitioning into

[†] Department of Chemical Engineering.
[‡] Department of Mechanical Engineering.

the carbon nanotube (CNT) pore, which is caused by the transfer of charged particles from a high-dielectric solvent (bulk water) to a low-dielectric environment (the interior of the CNT),[11] electrostatic binding to the negatively charged carboxylate groups near the pore mouth,[12] and the partial shedding of hydration shells for ions entering small, hydrophobic pores.[13]

The current trace under K^+ blocking conditions reveals several interesting details regarding the construction of the nanopore system. Three Coulter states are evident, indicating that this system corresponds to two parallel nanopores with approximately equal proton conductances (Figure 2c). These states are analyzed in more detail below. We also observe that this system *fail-closes* when the potential drops below the 700 mV threshold, as it clearly remains in the blocked state. This feature is unique to this nanopore system and indicates that the electrostatic barrier is higher for the exit region than the entrance. Such an imbalance can occur from unequal numbers of charged carboxylic acid groups at the two ends of the nanopore, a condition easily realized because of the small number of attachment sites at the two ends of the CNT.[9] Also, the functionalization of positively and negatively charged groups at opposite ends of the nanopore may have the potential to draw individual cations and anions in opposite directions. The fail-closed state is intriguing because it allows for the systematic trapping of molecules within the nanopore, whereby chemical reactions or further manipulation can be performed before their expulsion by cycling the potential above the threshold.

In Figure 2b, a short-dwell-time state is periodically observed in the two pore system, corresponding to the coincident blockage of two K^+ ions in each nanopore. Figure 2c confirms that this system demonstrates three Coulter states, with the short dwell time corresponding to the longest arrival time (or interval between observations). The three distinct current levels indicate specific states of SWNTs #1 and #2: #1 and #2 both blocked (state 1); #1 open and #2 blocked or #1 blocked and #2 open (state 2); #1 open and #2 open (state 3). The two pores have very similar magnitudes of blockade currents, so only three states can be distinguished (Figure S3).

This parallel nanopore system provided an opportunity to test the statistical nature of pore-blocking events at potentials above the threshold. Specifically, we asked whether the dynamics of this system are described by a three-state Markov chain (Figure S5). We applied three different voltages (800, 900, and 1000 mV), which generated the current traces and all-point histograms shown in Figure 3. Again, since two parallel SWNT nanopores were involved in ion transport, the all-points histogram should indicate four peaks except in the case where the intermediate state (one blocked, one unblocked) is degenerate (Figure S3). We found that the ratios of the three observed peaks in the all-points histogram are consistent with a simple Markov process. It should be noted that the completely closed state displays a large arrival time (18 s) with a short dwell time (0.07 s) in all three cases. This state is rare (probability = 0.02) because two K^+ must transport coincidentally in each nanopore for it to be observed. Using the relative ratios of the three peaks, we calculated the probabilities of pore blocking for SWNTs #1 and #2 and obtained the respective values 0.73 and 0.066 at 800 mV (Figure 3a), 0.78 and 0.019 at 900 mV (Figure 3b), and 0.67 and 0.006 at 1000 mV (Figure 3c).

It should be noted that increasing the electric field would be expected to decrease the dwell times of single-pore occupancy, since K^+ should translocate more rapidly. The coincident state in SWNT #2 decreased with increasing potential, as expected. However, the increasing electric field also appeared to affect the frequency of cation arrival at the negatively charged pore mouth. Since SWNT

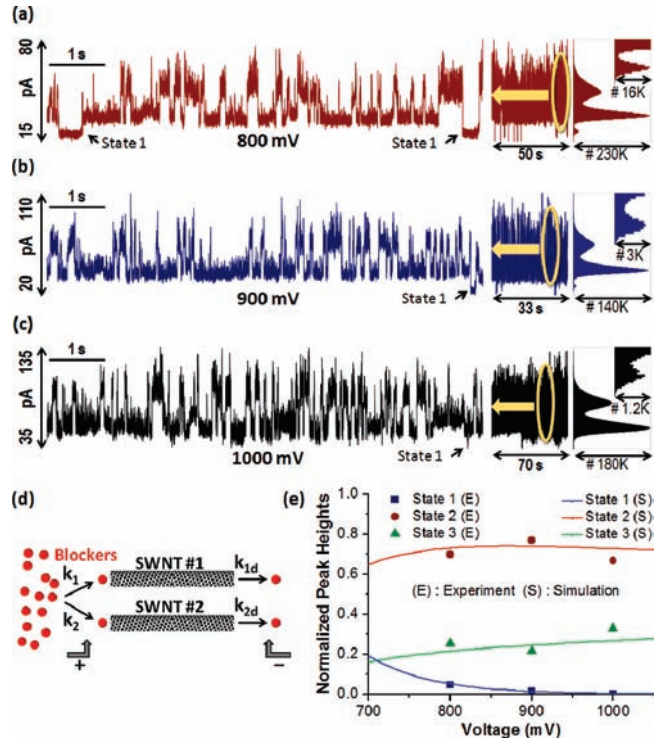

Figure 3. (a−c) Current traces and all-point histograms at (a) 800, (b) 900, and (c) 1000 mV. The insets show extended figures of state 1. Peak heights represent numbers of data points in states 1, 2, and 3. (d) Schematic illustration of transport of cations through SWNTs. The two SWNTs have different rate constants (k_1 and k_2, occupied by cations; k_{1d} and k_{2d}, releasing cations). (e) Comparison of the three states: simulation (solid curves) and experimental data at 800, 900, and 1000 mV (symbols).

#1 was affected by both the dwell time and this frequency, its probability was not inversely proportional to the electric field as one might have expected.

These distinct trends of SWNT #1 and #2 with applied voltage can be explained in terms of interference between the ion dwell time and the arrival frequency. The fast proton conduction through the SWNT[14,15] induces the depletion of the proton concentration at the pore mouth. Near the pore entrance, it gradually establishes a relatively high concentration of cations, which leads to pore blocking when a single cation enters the SWNT.[6,13] After the blocking cation translocates, this depletion process is repeated, and another cation continues the process. The frequency of this process is accelerated with increasing applied electric field, whereas the dwell time decreases. In SWNT #2 (low probability for blocking), occupancy of the SWNT by the cation is a relatively rare event, and the change in the arrival frequency with increasing applied voltage can be neglected in comparison with the change in dwell time. However, in SWNT #1 (high probability for blocking), the frequency of pore-blocking events appears to be sensitive to the applied electric field. Therefore, the probability is affected by both of the frequency of pore blocking events and the dwell time. In SWNT #1, the average dwell time decreased slightly as the applied voltage was increased (Figure S4b), whereas the frequency of pore blocking events increased. This difference can be caused by either the defects/impurities in the SWNTs, the various charge conditions[16] at the pore mouths of the SWNTs, or slight differences in diameters and chiralities.[17] For example, the ends of SWNTs etched by the oxygen plasma form carboxylic acid groups that may not be identically shaped on SWNTs #1 and #2.[9]

To further illustrate, we can describe the two ion channels analytically using a simple three-state Markov chain governed by

two different sets of rate constants (Figure 3d). The rate constants for cation blocking in SWNT #1 (k_1) and SWNT #2 (k_2) control the arrival times and depend on the statuses of the respective pore mouths. We note that pore blocking in #1 appears to be more frequent than in #2 ($k_1 > k_2$). The rate constants for the pore #1 (k_{1d}) and #2 (k_{2d}) should be known from the electric field and the scaling of ion mobility. The expected distribution of states 1, 2, and 3 (Figure S5) are then given by the following expressions:

$$\begin{aligned} P_1 &= p_{S1}p_{S2} \\ P_2 &= p_{S1} + p_{S2} - 2p_{S1}p_{S2} \\ P_3 &= (1 - p_{S1})(1 - p_{S2}) \end{aligned} \tag{1}$$

where P_j is the probability of state j ($j = 1-3$) and p_{S1} and p_{S2} are the pore-blocking probabilities for SWNTs #1 and #2, respectively, which can be described by cation-in (γ_1, γ_2) and cation-out (γ_{1d}, γ_{2d}) factors as follows:

$$\begin{aligned} p_{S1} &= \gamma_1(1 - \gamma_{1d}) \\ p_{S2} &= \gamma_2(1 - \gamma_{2d}) \end{aligned} \tag{2}$$

Each γ value can be calculated from the corresponding rate constant according to the expressions

$$\begin{aligned} \gamma_1 &= 1 - e^{-k_1 t} \\ \gamma_{1d} &= 1 - e^{-k_{1d} t} \\ \gamma_2 &= 1 - e^{-k_2 t} \\ \gamma_{1d} &= 1 - e^{-k_{2d} t} \end{aligned} \tag{3}$$

where t is the time interval for the observation. The rate constant for release of cations from SWNT #i can be estimated as

$$k_{id} = \frac{\mu_i(E - E_{th})}{L} \tag{4}$$

where L is the length of the SWNT, μ is the ion mobility of the SWNT, E is the applied voltage, and E_{th} is the threshold voltage. Figure 3e shows that the simulations of the relative peak heights closely correspond with the experimental results. The weight of state 1 rapidly decreases from the threshold voltage with increasing applied voltage, while that of state 3 slowly increases (Figure S6a,c). State 1 is dominated by pore blocking of SWNT #2, which is a rare event, so its weight depends on the ion mobility, which is inversely proportional to the voltage. State 3 shows a gradual increase because the increase in the frequency of pore blocking decays with decreasing ion mobility. Uniquely, the probability of state 2 increases for voltages up to 860 mV, the range over which the frequency increase surpasses the overall decrease in dwell time. However, the probability of state 2 decreases for voltages over 860 mV because the decrease in dwell time overcomes the effect of the rising frequency (Figure S6b). We conclude that a simple Markov network with a linear electric-field dependence of the translocation velocity approximately describes this system.

In conclusion, there is clearly a defined threshold voltage for cation partitioning into a SWNT ion channel. There is evidence that such nanopores can fail-close, meaning that pore blocking ceases upon a decrease in potential below the threshold, enabling schemes for molecular trapping. The case of two parallel ion channels, evidenced by three Coulter states with one being degenerate, is well-described using a simple three-state Markov network. An electric field and constant mobility are able to describe the behavior of the two-pore system parametrically in applied potential. This means that it should be possible to analytically describe and predict the behavior of such pore networks, enabling applications for molecular detection, separation, and catalysis in these unique nanopores.

Acknowledgment. The authors are grateful for funding from the Institute for Soldier Nanotechnology at the Massachusetts Institute of Technology, which is supported by the U.S. Army Research Office under Contract W911NF-07-D-0004, and for a fellowship to M.S.S from the Sloan Foundation. M.S.S is grateful for an Office of Naval Research Young Investigator Award as well as CAREER and PECASE Awards. W.C. acknowledges fellowship support from ILJU.

Supporting Information Available: Device fabrication, modeling of two-pore states and probability, extended current traces, and histograms of mobility and conductance. This material is available free of charge via the Internet at http://pubs.acs.org.

References

(1) Kowalczyk, S. W.; Hall, A. R.; Dekker, C. *Nano Lett.* **2010**, *10*, 324.
(2) Kowalczyk, S. W.; Tuijtel, M. W.; Donkers, S. P.; Dekker, C. *Nano Lett.* **2010**, *10*, 1414.
(3) Heng, J. B.; Aksimentiev, A.; Ho, C.; Marks, P.; Grinkova, Y. V.; Sligar, S.; Schulten, K.; Timp, G. *Nano Lett.* **2005**, *5*, 1883.
(4) Heng, J. B.; Ho, C.; Kim, T.; Timp, R.; Aksimentiev, A.; Grinkova, Y. V.; Sligar, S.; Schulten, K.; Timp, G. *Biophys. J.* **2004**, *87*, 2905.
(5) MacKinnon, R. *Angew. Chem., Int. Ed.* **2004**, *43*, 4265.
(6) Fornasiero, F.; Park, H. G.; Holt, J. K.; Stadermann, M.; Grigoropoulos, C. P.; Noy, A.; Bakajin, O. *Proc. Natl. Acad. Sci. U.S.A.* **2008**, *105*, 17250.
(7) Lee, C. Y.; Choi, W.; Han, J. H.; Strano, M. S. *Science* **2010**, *329*, 1320.
(8) Shao, Q.; Zhou, J.; Lu, L. H.; Lu, X. H.; Zhu, Y. D.; Jiang, S. Y. *Nano Lett.* **2009**, *9*, 989.
(9) Wong, S. S.; Joselevich, E.; Woolley, A. T.; Cheung, C. L.; Lieber, C. M. *Nature* **1998**, *394*, 52.
(10) Huang, S. M.; Cai, X. Y.; Liu, J. *J. Am. Chem. Soc.* **2003**, *125*, 5636.
(11) Peter, C.; Hummer, G. *Biophys. J.* **2005**, *89*, 2222.
(12) Joseph, S.; Mashl, R. J.; Jakobsson, E.; Aluru, N. R. *Nano Lett.* **2003**, *3*, 1399.
(13) Beckstein, O.; Tai, K.; Sansom, M. S. P. *J. Am. Chem. Soc.* **2004**, *126*, 14694.
(14) Dellago, C.; Naor, M. M.; Hummer, G. *Phys. Rev. Lett.* **2003**, *90*, 105902.
(15) Holt, J. K.; Park, H. G.; Wang, Y. M.; Stadermann, M.; Artyukhin, A. B.; Grigoropoulos, C. P.; Noy, A.; Bakajin, O. *Science* **2006**, *312*, 1034.
(16) Majumder, M.; Zhan, X.; Andrews, R.; Hinds, B. J. *Langmuir* **2007**, *23*, 8624.
(17) Won, C. Y.; Joseph, S.; Aluru, N. R. *J. Chem. Phys.* **2006**, *125*, 114701.

JA108011G